



# Detection Opportunity for Aromatic Signature in Titan's Aerosols in the 4.1–5.3 $\mu\text{m}$ Range

Christophe Mathé<sup>1</sup> , Thomas Gautier<sup>2</sup>, Melissa G. Trainer<sup>3</sup>, and Nathalie Carrasco<sup>2,4</sup> 

<sup>1</sup> LESIA, Observatoire de Paris, Université PSL, CNRS, Sorbonne Université, Univ. Paris Diderot, Sorbonne Paris Cité, 5 place Jules Janssen, 92195 Meudon, France  
[christophe.mathe@obspm.fr](mailto:christophe.mathe@obspm.fr)

<sup>2</sup> LATMOS, CNRS, Université Versailles St-Quentin, Sorbonne Université, Université Paris-Saclay, 11 Bvd d'Alembert F-78280 Guyancourt. France  
[thomas.gautier@latmos.ipl.fr](mailto:thomas.gautier@latmos.ipl.fr)

<sup>3</sup> NASA Goddard Space Flight Center, 8800 Greenbelt Road, Greenbelt MD, USA

<sup>4</sup> Institut Universitaire de France, France

Received 2018 May 29; revised 2018 June 21; accepted 2018 June 27; published 2018 July 13

## Abstract

The *Cassini/Huygens* mission provided new insights on the chemistry of the upper atmosphere of Titan. The presence of large molecules and ions ( $>100$ 's of amu) detected by *Cassini* at high altitude was not expected, and questions the original assumptions regarding the aerosol formation pathways. From recent laboratory studies, it has been shown that the inclusion of trace amounts of aromatic species drastically impacts the chemistry of aerosol formation and induces observable changes in the properties of the aerosols. In this Letter we focus on the effect of one of the simplest nitrogenous aromatics, pyridine ( $\text{C}_5\text{H}_5\text{N}$ ), on the infrared signature of Titan's aerosol analogs. We introduce initial gas mixtures of (i)  $\text{N}_2\text{-C}_5\text{H}_5\text{N}$  (100%/250 ppm), (ii)  $\text{N}_2\text{-CH}_4\text{-C}_5\text{H}_5\text{N}$  (99%/1%/250 ppm), and (iii)  $\text{N}_2\text{-CH}_4$  (99%/1%) in a cold plasma discharge. The material produced, herein called tholins, is then analyzed by mid-infrared spectroscopy. When adding pyridine in the discharge, the tholins produced present an aromatic signature in the 4.1–5.3  $\mu\text{m}$  ( $1850\text{--}2450\text{ cm}^{-1}$ ) spectral region, attributed to overtones of aromatic C–H out-of-plane bending vibrations. We also observe a spectral shift of the nitrile and iso-nitrile absorption band with the inclusion of pyridine in the gas mixture. These results could help to investigate the data obtained at Titan by the *Cassini/Visual and Infrared Mapping Spectrometer* (VIMS) instrument in the 1–5  $\mu\text{m}$  infrared window.

**Key words:** astrochemistry – infrared: planetary systems – methods: laboratory: solid state – planets and satellites: atmospheres – solid state: refractory

## 1. Introduction

The largest moon of Saturn, Titan, has fascinated numerous scientists because it is the only moon in our solar system that possesses an atmosphere. Titan's atmosphere is composed of nitrogen ( $\sim 98\%$ ), methane ( $\sim 1.5\%$ ), and traces species of hydrocarbons (Waite et al. 2005). In the ionosphere ( $\sim 1000\text{ km}$ ), gas is dissociated and ionized by solar photon irradiation and energetic particles from Saturn's magnetosphere. This chemistry leads to the formation of complex photochemical aerosols in the atmosphere. Since the discovery of Titan's thick haze layer by the *Voyager* probe (Smith et al. 1981), the question of the aerosol composition has been widely investigated (Khare et al. 1984; Imanaka et al. 2004; Gautier et al. 2012). The results from the *Cassini/Huygens* mission have provided constraints on the chemical composition of the aerosol, though not a comprehensive analysis (Hörst 2017). Results from the *Huygens/Aerosol Collector Pyrolyser* (ACP) experiment demonstrated that the atmospheric aerosols incorporate a large fraction of nitrogen (Israel et al. 2005). *Cassini/Composite Infrared Spectrometer* (CIRS) detected C–H bending mode in the aerosol signature in the far-infrared (far-IR; Vinatier et al. 2012).

However, aromaticity in Titan's aerosol remains uncertain. Dinelli et al. (2013) reported a detection of an unidentified emission around 3.28  $\mu\text{m}$  ( $3049\text{ cm}^{-1}$ ) in Titan's atmosphere, observed by the Visual and Infrared Mapping Spectrometer (VIMS) instrument on board *Cassini*. Based on the in situ measurements of small molecules by Ion and Neutral Mass Spectrometer (INMS), the feature could be attributed to aromatic molecules like benzene (Waite et al. 2007). Yet, the small

concentration of benzene (few ppm) did not explain the large magnitude of the emission peak observed by VIMS. Dinelli et al. (2013) suggested that the unidentified emission could be due to a solid signature of polycyclic aromatic hydrocarbons (PAHs) or heterocyclic aromatic compounds in the Titan's upper atmosphere (Coates et al. 2007; Waite et al. 2007). López-Puertas et al. (2013) further attempted to compare this unidentified emission peak to PAH emission features. PAHs have their vibrational signatures in the spectral range of the unidentified emission. Moreover, PAHs excited by UV-solar radiation redistribute internally the energy in their vibrational modes, causing near and mid-infrared (mid-IR) emissions. To analyze this unidentified emission, VIMS observations were compared to an excitation model of a set of PAHs and polycyclic aromatic nitrogen heterocycles (PANHs). The observed spectral feature from VIMS was found to be consistent with the combination of several PAH spectra. López-Puertas et al. (2013) established a list of the 19 most abundant PAHs fitting well with the VIMS observations and composed of 10–11 aromatics rings on average. This attribution is not unique or univocal, but provides strong evidence that there may be an aromatic component in Titan's aerosols.

In this Letter we investigate the infrared spectra of aerosol analogs with a high aromatic content with the aim of identifying new features that would be indicators the aromatic component of Titan's aerosols. To produce such highly aromatic aerosols, we begin with trace amounts of pyridine ( $\text{C}_5\text{H}_5\text{N}$ ). Indeed, previous laboratory investigations by Sebree et al. (2014) showed that aerosols produced with trace amounts of 1- and 2-ring aromatics provided the best match to broad

aerosol emission features below  $200\text{ cm}^{-1}$  actually, observed at Titan in CIRS far-IR spectra (Anderson & Samuelson 2011). Aerosol analogs with a nitrogen component, including those formed with pyridine, provided the strongest feature in this region of the spectrum. Here, pyridine is chosen in order to favor a high nitrogen content, consistently with the *Huygens*/ACP detection (Israel et al. 2005), and because this compound has been inferred from INMS data to be present in the upper atmosphere (Vuitton et al. 2007).

A typical signature for aromaticity would be the fingerprints due to the  $\nu_{(0-1)}$  transition of the out-of-plane C–H bending modes, which are usually located in the  $600\text{--}900\text{ cm}^{-1}$  wavenumber range (Tommasini et al. 2016). However, this region is generally crowded for hydrocarbons (Coustenis et al. 2010), making it challenging to decipher in complicated spectra. Fortunately, such fingerprints have a counterbalance due to aromatic overtones linked to the  $\nu_{(0-3)}$  transition in the  $1800\text{--}2100\text{ cm}^{-1}$  wavenumber range, which happens to be a region of the spectrum free from any other vibrational absorptions (Herzberg 1950). We thus choose to investigate this spectral band, which partially coincides with a *Cassini*/VIMS observable range ( $1\text{--}5\text{ }\mu\text{m}$ ) (Brown et al. 2005), to characterize the spectra of our laboratory aerosols (Brown et al. 2005).

## 2. Experimental Details

Aerosols analogs were produced using the Production d’Aérosols en Microgravité par Plasma REactifs (PAMPRE) experiment, based on a plasma discharge in a gas mixture of nitrogen with methane and/or pyridine. Then, the tholins produced are extracted from the reactor to be analyzed by infrared spectroscopy with an attenuated total reflection (ATR) method.

The PAMPRE setup is based on a capacitively coupled radio-frequency ( $13.6\text{ MHz}$ ) system as energy source to induce a plasma in gas mixtures. The experimental details can be found in Szopa et al. (2006).

The gas mixture is injected into the top of the vacuum reactor at a  $55\text{ sccm}$  (standard cubic centimeter per second) flow rate. The PAMPRE reactor is operated at room temperature, at a pressure of  $0.9\text{ mbar}$  and an effective power of  $30\text{ W}$ .

When the reactor is on, the plasma induces chemistry that leads to the formation of organic aerosol, considered analogs of Titan’s haze particulates. Due to charge effects, aerosols are maintained in levitation in the plasma, allowing for growth in the free atmosphere without induced wall effects. The aerosol formation process is self-limiting. Once the solid particles reach a critical diameter they become too heavy, and the electric field yields and the gravitation forces take over. The particles fall through the grid and deposit outside of the reactor for collection on a glass vessel. These solid products are called tholins. An estimate of the production rate, defined as the ratio between the mass of tholins produced and the production duration, is obtained by weighing the total collected sample with a  $0.1\text{ mg}$  precision scale. This estimate only corresponds to the lower limit of the production rate, as a few tholins remain on the glass vessel due to electrostatic charging and cannot be extracted. The detailed protocol and a discussion on the limitations of this procedure, together with a study on the influence of methane percentage on tholins production rate in the PAMPRE reactor, can be found in Sciamma-O’Brien et al. (2010).

**Table 1**  
Initial Composition of the Gas Mixtures

Initial Gas Mixture	N <sub>2</sub> (%)	CH <sub>4</sub> (%)	C <sub>5</sub> H <sub>5</sub> N (ppm)
N <sub>2</sub> –CH <sub>4</sub>	99	1	0
N <sub>2</sub> –CH <sub>4</sub> –C <sub>5</sub> H <sub>5</sub> N	~99	1	250
N <sub>2</sub> –C <sub>5</sub> H <sub>5</sub> N	~100	0	250

Here, three different gas mixtures were used to produce aerosols as presented in Table 1: (1) a reference case with only N<sub>2</sub> and CH<sub>4</sub> in the initial gas mixture, (2) a second case to evaluate the effect of traces of pyridine in addition to CH<sub>4</sub> to compare to the reference mix, and (3) a third case to evaluate the capacity of pyridine itself to generate aerosols with a highly aromatic signature.

To test the effect of pyridine in the N<sub>2</sub>–CH<sub>4</sub> chemical system, we have chosen to set the methane concentration at 1% in our experiments, in agreement with a lower limit for Titan’s atmospheric composition (Niemann et al. 2010).

Experiments were made using reactants from Air Liquide: N<sub>2</sub> (>99,999% purity), a certified CH<sub>4</sub>/N<sub>2</sub> mixture (10% CH<sub>4</sub>, >99,999% purity), and a certified pyridine/N<sub>2</sub> mixture (550 ppm of pyridine, >95% purity).

The ATR method enables a direct measurement of the infrared spectra of solid product without further preparation. For this analysis a few micrograms of bulk tholins are deposited onto the ATR plate of a Nicolet 6700 Fourier Transform InfraRed—ATR from Thermo Fisher Scientific. Spectra were recorded on the  $1800\text{--}2500\text{ cm}^{-1}$  wavenumber range with a  $2\text{ cm}^{-1}$  spectral resolution and a Michelson velocity set at  $0.624\text{ cm}^{-1}\text{ s}^{-1}$ . All spectra were normalized to the most intense peak around  $2169\text{ cm}^{-1}$  and corrected for atmospheric background.

## 3. Results and Discussion

### 3.1. Aerosol Production Efficiency

Rough estimates of the production rates were measured for the two experiments performed with 250 ppm of pyridine, with and without methane. For a similar plasma duration of 6 hr, we found a mass production of 70 and 8.2 mg with and without methane, respectively. The production rate in the presence of 1% methane is an order of magnitude larger ( $11.7\text{ mg/h}$  and  $1.4\text{ mg/h}$ , respectively), but needs to be scaled to consider the relative amount of carbon introduced in the two experiments. Each molecule of pyridine contains five carbon atoms, so the 250 ppm of pyridine provides 1250 ppm carbon atoms to the reactive mixture. There is, therefore, one order of magnitude less carbon provided by 250 ppm pyridine than by 1% methane amount in the discharge. Thus, the methane and the aromatic pyridine have roughly the same efficiency to produce solid particles in the plasma experiment. This suggests that on Titan a few ppm of aromatic molecules could contribute significantly to the aerosol formation, especially at altitudes where methane photochemistry is no longer active. This is consistent with previously reported studies (Trainer et al. 2013, Sebree et al. 2014).

### 3.2. Aerosol Spectral Signature

The spectra of the three samples in the  $1850\text{--}2450\text{ cm}^{-1}$  range are shown in Figure 1.

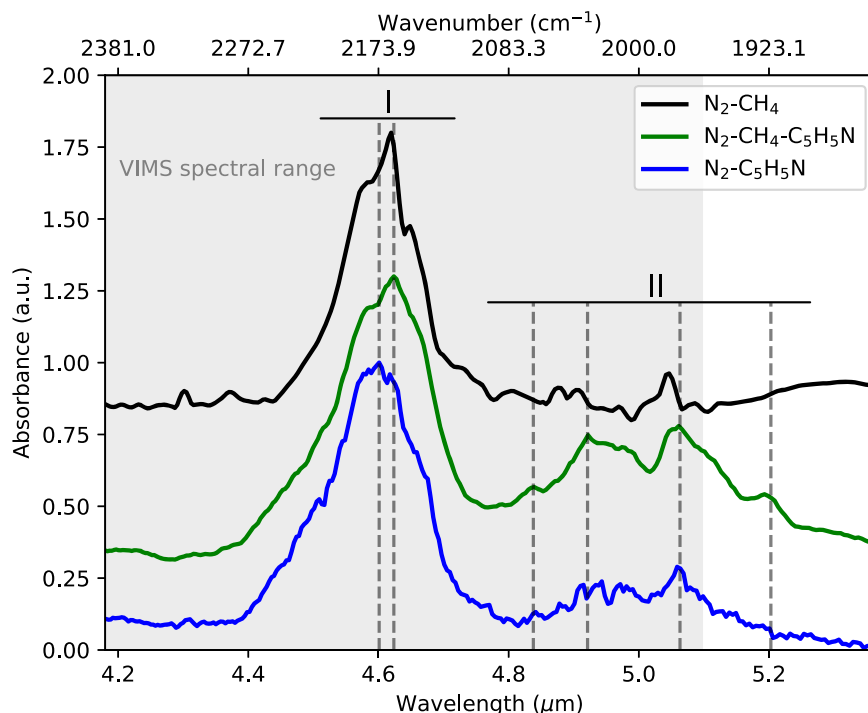


**Figure 1.** Infrared spectra of tholins in the 4.1–5.3  $\mu\text{m}$  spectral range (1850–2450  $\text{cm}^{-1}$ ). The curves are labeled with the initial gas mixture used to produce tholins (see Table 1):  $\text{N}_2\text{-CH}_4$  (black curve),  $\text{N}_2\text{-C}_5\text{H}_5\text{N}$  (blue curve), and  $\text{N}_2\text{-CH}_4\text{-C}_5\text{H}_5\text{N}$  (green curve). Regions I and II correspond to nitrile vibration and aromatic overtones, respectively. The gray corresponds to the VIMS spectral range.

Two features stand out in this range of the spectra: one region between 2100 and 2250  $\text{cm}^{-1}$  (zone I), and the second between 1900 and 2100  $\text{cm}^{-1}$  (zone II). For each region, the band center position, intensity, and potential attribution are detailed in Table 2.

Zone I corresponds to the well-known absorption bands due to the nitrile (R-CN) and iso-nitrile (R-NC) functions (Imanaka et al. 2004; Gautier et al. 2012). When comparing the three spectra in Figure 1, the first aspect of note is the similarity in position of this feature. It is dominated by an absorption band peaking at 2173  $\text{cm}^{-1}$  corresponding to the stretching mode of nitrile or iso-nitrile terminal functions branched on aliphatic structures.

However, a second contribution appears in this broad band, peaking at around 2240  $\text{cm}^{-1}$  (see peaks attribution in Table 2). The weight of this contribution is strongest in the  $\text{N}_2\text{-C}_5\text{H}_5\text{N}$  spectrum, becoming a clear shoulder on the band at 2173  $\text{cm}^{-1}$  (blue curve in Figure 1). The shift to a higher wavenumber is consistent with the signature of nitrile functionalities branched on aromatic rings (Sciamma-O’Brien et al. 2017).

The absorption features in zone I are consistent with the formation of nitrile and iso-nitrile functions, primarily branched from aliphatic structures, for the three tholins samples—even in the experiment with only pyridine as the carbon source. However, some of the nitrile and iso-nitrile functional groups may also be branched from aromatic rings, as suggested by the contribution of a signature at around 2240  $\text{cm}^{-1}$ . This signature is especially prominent in the samples produced with pyridine.

Zone II shows a new band appearing between 1900–2100  $\text{cm}^{-1}$  in the spectra of samples produced with pyridine. Four main peaks can be distinguished within the  $\text{N}_2\text{-CH}_4\text{-C}_5\text{H}_5\text{N}$  (green curve) at positions 1922, 1973, 2026, and 2074  $\text{cm}^{-1}$ . These bands have also been observed in recent

work by Sciamma-O’Brien et al. (2017) in tholins produced with mixtures of nitrogen, methane, and benzene.

This spectral region does not match with any fundamental vibration of organic chemical functional groups, but we can confidently attribute them to aromatic derivatives overtones ( $\nu_{0-3}$ ) because of the following.

1. A recent simulation study on the fundamental fingerprints ( $\nu_{0-1}$ ) of 51 pure PAHs has shown the spectral region between 730 and 910  $\text{cm}^{-1}$  corresponds to out-of-plane CH bending at the edge of the aromatic cycle (Tommasini et al. 2016).
2. Overtone signatures are due to the  $n$  harmonic of the fundamental vibrational state ( $\nu_{0-1}$ ) of a molecule, corresponding to the  $\nu_{0-n}$  transition (Young et al. 1951; Kendall 1966).
3. The frequencies of overtones do not correspond exactly to  $n$ -times the frequency of the fundamental vibration, but rather are expected to show some shift toward a lower wavenumber due to the anharmonicity of molecules (Herzberg 1950).
4. Gautier et al. (2017) also reported the detection of polymeric patterns in the mass spectra of tholins produced with gas mixture of nitrogen, methane, and one or two rings aromatics. These were interpreted as a possible signature of aromatic functions within the structure of tholins produced in such a gas mixture.

The detection of these C–H out-of-plane bending at the edge of the aromatic cycle overtones, in a region free of fundamental vibration of any other organic chemical functional groups, confirms the inclusion of aromatic cycles in the macromolecular structure of our tholins and provides a first observational opportunity for the determination of aromatic content of Titan’s aerosols.

**Table 2**  
List of the Absorption Bands Detected in the 4.1–5.3  $\mu\text{m}$  Spectral Range

Region	$\text{N}_2\text{-CH}_4$		$\text{N}_2\text{-C}_5\text{H}_5\text{N}$		$\text{N}_2\text{-CH}_4\text{-C}_5\text{H}_5\text{N}$		Potential Attributions
	Center $\mu\text{m}$ ( $\text{cm}^{-1}$ )	Intensity	Center $\mu\text{m}$ ( $\text{cm}^{-1}$ )	Intensity	Center $\mu\text{m}$ ( $\text{cm}^{-1}$ )	Intensity	
I	4.65 (2151)	m	4.68 (2137)	m	4.66 (2145)	w	$-\text{N}=\text{C}=\text{N}-$ (l), $-\text{CN}$ (m)
	4.62 (2164)	vs	4.60 (2173)	vs	4.62 (2163)	vs	Conjugated $-\text{CN}$ , such as $-\text{C}=\text{C}(-\text{NH}_2)$ (l), $\text{C}-\text{NC}$ stretching (l), $-\text{NC}$ (m), $\text{C}_{\text{ar}}-\text{CN}?$
	...	...	4.52 (2210)	w	4.54 (2204)	w	$\text{C}_{\text{ar}}-\text{NC}?$
	4.48 (2230)	w	4.48 (2233)	m	4.47 (2235)	w	$\text{R}-\text{NC}$ stretching (l), $-\text{N}=\text{C}=\text{N}-$ (m)
II	...	...	...	...	5.20 (1922)	m	Overtone $\text{C}-\text{H}$ (solo)
	5.05 (1980)	vw	5.06 (1977)	w	5.06 (1975)	s	Overtone $\text{C}-\text{H}$ (duo)
	...	...	4.94 (2025)	w	4.92 (2032)	s	Overtone $\text{C}-\text{H}$ (trio)
	...	...	4.89 (2045)	vw	4.84 (2067)	w	Overtone $\text{C}-\text{H}$ (quatro)

**Note.** Potential attribution of peaks in regions I are taken from (1) Imanaka et al. (2004) and (2) Gautier et al. (2012). Band intensity legend: vs = very strong; s = strong, m = medium, w = weak, vw = very weak.

Thus, we suggest that the observation of these bands, which could be partially detectable in the *Cassini*/VIMS-infrared (IR) observational range, would provide the strongest indication yet regarding the aromaticity of Titan's aerosols.

#### 4. Conclusion

In this Letter we have identified a strongly indicative signature of aromaticity of Titan's aerosol analogs in the 4.3–5.1  $\mu\text{m}$  spectral range. This signature is attributed to overtones of the aromatic structural vibrations of the aerosols. The latter frequencies correspond to out-of-plane bending vibrations in the 11.7–15.4  $\mu\text{m}$  spectral range. Two instruments on *Cassini* have been able to observe the Titan atmosphere at these wavelengths. The fingerprint frequencies would be in the FP3 window of the CIRS instrument, and were tentatively reported by Vinatier et al. (2012) with a signature at 13.25  $\mu\text{m}$ . The corresponding overtones would be within the VIMS-IR spectral range.



Regarding a search for an aromatic signature in Titan's aerosols, our results indicate that targeting the overtones in the existing VIMS-IR data and the fingerprint frequencies in the CIRS-FP3 window would provide a strategy for complementary detections.

Our work, therefore, provides a new detection opportunity for aromatic signature in Titan's aerosols using the 4.1–5.3  $\mu\text{m}$  range of the VIMS-IR instrument. Such a detection could provide the most convincing evidence of the possible aromaticity of Titan's aerosols. The aromatic or aliphatic nature of Titan's aerosols is an important issue, as these functionalities affect optical properties and chemical activity. A significant aromatic component in the aerosol would induce a different fate of the aerosols both in the atmosphere and on Titan's surface, for example regarding their reactivity at low altitude or on the surface (Gudipati et al. 2013) and their respective solubility in Titan's lakes (Cable et al. 2012; Malaska & Hodyss 2014; Chevrier et al. 2015).

C.M. wishes to thank the Paris Observatory for its financial support for this work. N.C. thanks the European Research Council for its financial support under the ERC PrimChem project (grant agreement No. 636829). M.G.T. thanks the NASA Solar System Workings Program for financial support.

The authors thank Fabrice Duvernay for the fruitful discussion on the anharmonicity of overtones signatures.

#### ORCID iDs

Christophe Mathé  <https://orcid.org/0000-0002-2905-9001>  
Nathalie Carrasco  <https://orcid.org/0000-0002-0596-6336>

#### References

- Anderson, C. M., & Samuelson, R. E. 2011, *Icar*, **212**, 762  
Brown, R. H., Baines, K. H., Bellucci, G., et al. 2005, *SSRv*, **115**, 111  
Cable, M. L., Hörst, S. M., Hodyss, R., et al. 2012, *Chem. Rev.*, **112**, 3  
Chevrier, V. F., Luspay-Kuti, A., & Singh, S. 2015, *LPSC*, **1832**, 2763  
Coates, A. J., Cray, F. J., Lewis, G. R., et al. 2007, *GeoRI*, **34**, L22103  
Coustenis, A., Jennings, D. E., Nixon, C. A., et al. 2010, *Icar*, **207**, 461  
Dinelli, B. M., López-Puertas, M., Adriani, A., et al. 2013, *GeoRI*, **40**, 1489  
Gautier, T., Carrasco, N., Mahjoub, A., et al. 2012, *Icar*, **221**, 320  
Gautier, T., Sebree, J. A., Li, X., et al. 2017, *P&SS*, **140**, 27  
Gudipati, M. S., Jacovi, R., Couturier-tamburelli, I., Lignell, A., & Allen, M. 2013, *NatCo*, **4**, 1648  
Herzberg 1950, *Molecular Spectra and Molecular Structure* (New York: Van Nostrand Reinhold)  
Hörst, S. M. 2017, *JGRE*, **122**, 432  
Imanaka, H., Khare, B. N., Elsila, J. E., et al. 2004, *Icar*, **168**, 344  
Israël, G., Szopa, C., Raulin, F., et al. 2005, *Natur*, **438**, 796  
Kendall 1966, *Applied Infrared Spectroscopy* (New York: Van Nostrand Reinhold)  
Khare, B. N., Sagan, C., Arakawa, E. T., et al. 1984, *Icar*, **60**, 127  
López-Puertas, M., Dinelli, B. M., Adriani, A., et al. 2013, *ApJ*, **770**, 132  
Malaska, M. J., & Hodyss, R. 2014, *Icar*, **242**, 74  
Niemann, H. B., Atreya, S. K., Demick, J. E., et al. 2010, *JGRE*, **115**, E12006  
Sciamma-O'Brien, E., Carrasco, N., Szopa, C., Buch, A., & Cernogora, G. 2010, *Icar*, **209**, 704  
Sciamma-O'Brien, E., Upton, K. T., & Salama, F. 2017, *Icar*, **289**, 214  
Sebree, J. A., Trainer, M. G., Loeffler, M. J., & Anderson, C. M. 2014, *Icar*, **236**, 146  
Smith, B. A., Soderblom, L., Beebe, R., et al. 1981, *Sci*, **212**, 163  
Szopa, C., Cernogora, G., Boufendi, L., Correia, J. J., & Coll, P. 2006, *P&SS*, **54**, 394  
Tommasini, M., Lucotti, A., Alfè, M., Ciajolo, A., & Zerbi, G. 2016, *AcSpA*, **152**, 134  
Trainer, M. G., Sebree, J. A., Yoon, Y. H., & Tolbert, M. A. 2013, *ApJL*, **766**, L4  
Vinatier, S., Rannou, P., Anderson, C. M., et al. 2012, *Icar*, **219**, 5  
Vuitton, V., Yelle, R. V., & Mcewan, M. J. 2007, *Icar*, **191**, 722  
Waite, J. H., Niemann, H. B., Yelle, R. V., et al. 2005, *Sci*, **308**, 982  
Waite, J. H., Young, D. T., Cravens, T. E., et al. 2007, *Sci*, **316**, 870  
Young, C. W., Du Vall, R. B., & Wright, N. 1951, *AnaCh*, **2**, 1